Jurnal Ilmu Fisika
Vol. 17, No. 1, March 2025, pp. 41–52
ISSN: 1979-4657 (Print); 2614-7386 (Online)
https://doi.org/10.25077/jif.17.1.41-52.2025

Jurnal Ilmu Fisika
Open Access

Identification of the Presence of Pumice Stone Based on Georadar Data and Geoelectric Resistivity Data in Ampenan District and Sekarbela District, Mataram City

Sefti Dini Arsi, Muhammad Farid, Refrizon Refrizon
Department of Physics, Bengkulu University, Bengkulu, 38371, Indonesia

Article Info

Article History:

Received October 0[illegible], 2024
Revised January 28, 2025
Accepted February 01, 2025
Published online February 23, 2025

Keywords:

Pumice Stone
Georadar
Geoelectric Resistivity
Mount Samalas

Corresponding Author:

Muhammad Farid,
Email: mfarid@unib.ac.id

ABSTRACT

This study was conducted to identify the presence and distribution of pumice resulting from the 1257 AD eruption of Mount Samalas in the Ampenan and Sekarbela Districts of Mataram City. The research is significant because pumice serves as a volcanic indicator that greatly influences soil characteristics and the local environment. The study aims to map the distribution of pumice and to examine its subsurface dispersal, particularly in coastal areas. Georadar and geoelectric resistivity methods were employed—two geophysical techniques that measure the electrical response of the subsurface, thereby detecting changes in resistivity and conductivity indicative of volcanic material such as pumice. The results reveal that pumice is uniformly distributed at depths of 0–9 meters and is intermixed with gravel, silt, and sand. In the study area, the soil layer is predominantly sandy, likely due to its coastal location. This research underscores the importance of using geophysical methods to map the distribution of volcanic materials in shallow layers, especially in areas affected by volcanic eruptions.

1. INTRODUCTION

The eruption of Mount Samalas was the largest volcanic eruption in Indonesia, and it occurred in 1257 AD. The size of this eruption is estimated to reach 7 VEI scale. It was recorded that the height of Mount Samalas' eruption column reached 43 km (Lavigne et al., 2013). This eruption produced pyroclastic material, most of which flowed north while the rest flowed south and then branched into two. One branch flows southeast for 30 km across what is now Selong City and the second branch flows southwest for 40 km across the area that includes Mataram City (Wahidah et al., 2016). The direction of flow of pyroclastic material can be seen more clearly in Figure 1. The presence of pumice characterizes the pyroclastic material resulting from the eruption of Mount Samalas (Lavigne et al., 2013). Therefore, pumice stone is very abundant in Lombok.

It can be done using geophysical methods, including the georadar method and the geoelectric resistivity method, to determine the presence of pumice stone. Both methods utilize the electrical response of subsurface materials but with different approaches. The georadar method uses electromagnetic waves to detect reflections due to changes in electromagnetic conductivity in subsurface materials (Narotama Sarjan & Muchtaranda, 2023), while the geoelectric method uses electric current to measure the resistivity of subsurface materials based on the distribution of the resulting electrical potential (Tranggono et al., 2024). Conductivity and resistivity are physical parameters that describe the ability of a material to conduct and inhibit the flow of electric current (An[illegible]n et al., 2023). These two parameters have an inverse relationship; if a material has high conductivity then its resistivity is low, and vice versa. Combining these two methods can reduce uncertainty in the interpretation of subsurface images (Paembonan et al., 2021).

Several studies related to pumice have been carried out in locations suspected to be routed for the flow of pyroclastic material, including in the Sembalun, Gangga, Ijobalit, and Lingsar Caldera areas. Figure 1 also shows pyroclastic flows across Mataram City. However, further study regarding the presence of pumice in Mataram City has never been carried out.

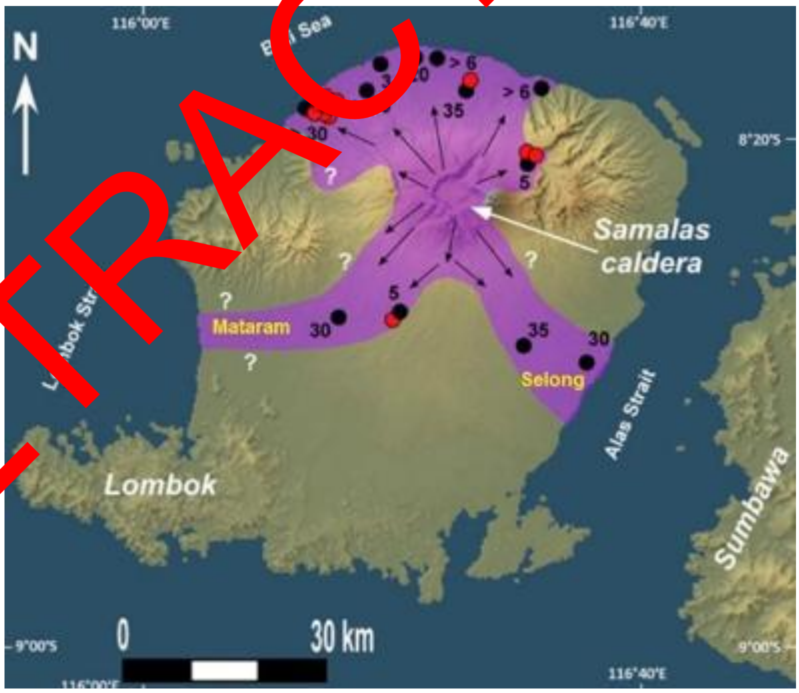

Figure 1. Pyroclastic Material Explosion Direction Map.

The strategic location as a place to investigate the presence of pumice in Mataram City is Ampenan and Sekarbela Districts. These two sub-districts are low-lying and close to the coast, making them strategic locations for investigating pumice deposition which may be widespread due to pyroclastic flows. Pumice produced by large eruptions can float on water and be carried by ocean currents to various coastal locations. Ampenan and Sekarbela as coastal areas are likely to receive large amounts of pumice due to the Samalas eruption. In connection with this, research has been carried out in Ampenan and Sekarbela Districts to determine the presence and distribution of pumice from the Samalas eruption based on the results of georadar data processing and geoelectric resistivity.

Lavigne et al., (2013), examine the large eruption of Mount Samalas in Lombok in 1257 AD, which produced extensive pyroclastic flows and large quantities of pumice. Ronodirdjo et al., (2020) carried out stratigraphic analysis to study volcanic sediment layers in the Ganges area, North Lombok. The analysis focused on layers of pumice found in outcrops of sand layers in local quarries. The research results revealed that Mount Samalas experienced three large eruptions, marked by layers of pumice which had three different colors, namely white, pink, and yellow. The white (13th century) and pink (500 BC) layers are the result of the most recent large eruption, while the yellow layer is the deepest and oldest layer.

Geophysical methods have been widely used to detect and map the presence of pumice, such as research conducted by Ustina et al., (2020), using the geoelectric method to analyze the thickness of the pumice layer as a function of source distance in Lingsar District. The research results show that the pumice layer is 10 – 21 meters thick. Meanwhile, laboratory measurements results show that the resistivity value for wet pumice is 23.9 – 40.0 Ωm and 204.3 – 354.8 Ωm for dry pumice. The thickness of the pumice layer decreases exponentially with distance from the eruption source. A study using geoelectric methods has also been carried out by Ustina et al., (2020), to determine the depth, thickness, and volume of pumice deposits resulting from the Samalas eruption in the Sembalun Caldera. The research results show that the resistivity value of the pumice layer is [illegible]4 – [illegible]51.49 Ωm at a depth of 1 – 21 meters, with a thickness ranging from 12 – 19 meters and an estimated volume of 56,201,780 m^3.

A study was conducted by Malawani et al. (20[illegible]) to investigate the subsurface layers in Mataram by conducting a stratigraphic survey and assisted by measurements using the ERT method to complete the stratigraphic data. Drilling data helps interpret resistivity values for various types of sediment. In this study, the sediment layer containing dry pumice material had a resistivity value of $\geq 300\ \Omega m$; on shallow water surfaces, the pumice layer had a resistivity value ranging from 30 – 300 Ωm. One of the tracks became a drilling location, and a mixture of pumice and sand was obtained at 2 – 12 m depth. Sudrajat et al. (2017) conducted drilling tests on Jalan Antareja, Cakranegera, and Mataram. Drilling depth up to 21 meters. Pumice stone is found at a depth of 1 – 9 meters, mixed with layers of sand, black sand, fine sand, and tuff.

The use of the georadar method to determine subsurface layers has been carried out by Ibrahim et al., (2019). The results obtained from using a tool with an antenna frequency of 250 MHz are at a depth ranging from 8 meters – 1[illegible] meters; there are two layers, namely top soil with a thickness of 1-2 meters and sand with a thickness of 11-13 meters with a small dielectric contrast value. (Vinod, 2014) also uses radar methods to investigate subsurface layers. The study results show that the research area consists of a concrete layer at a depth of 0.2 – 2.2 meters, a sandstone layer at a depth of 2.2 – ± 26 meters, and a layer of tuff layers between 5 – 34 meters. Based on several studies above, it is known that geophysical methods using georadar and geoelectric data processing can identify types of subsurface layers, including pyroclastic deposits resulting from volcanic eruptions.

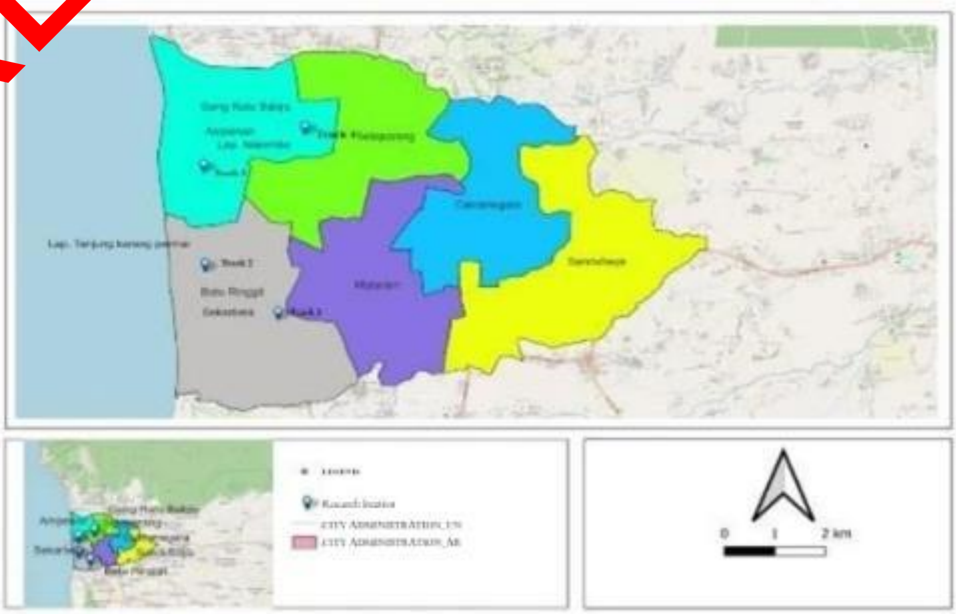

Figure 2. Study Location Map.

2. METHOD

This study was carried out from June 2024 to August 2024. The georadar data used in this study is secondary data obtained through collaboration between the Physics Study Program, FMIPA, Mataram University and the Physical Geography Laboratory, Paris 1 University, France. Data collection was carried out in Ampenan District and Sekarbela District in 2015, with a total of 4 measurement points. The study utilized a GPR system with a 250 MHz antenna frequency which provides an optimal balance between penetration depth (8-13 meters) and resolution. Meanwhile the geoelectric resistivity data used is primary data obtained from acquisition results at the same location as the georadar data collection location. Figure 2 shows a map of georadar and geoelectric data collection locations. In detail, the data collection locations can be seen in Table 1.

Table 1 Georadar and Geoelectric Data Collection Locations.

Location Coordinates	Location Code	Regional Name
-8°36'3,6"S 116°5'19,68"E	Track 1	Karang Pule Field , Sekarbela
-8°35'36,96"S 116°4'33,24"E	Track 2	Kuburan Cina, Sekarbela
-8°35'0,96"S 116°4'27,48"E	Track 3	Pengghulu Agung, Ampenan
-8°34'7,68"S 116°5'6,72"E	Track 4	Pejeruk, Ampenan

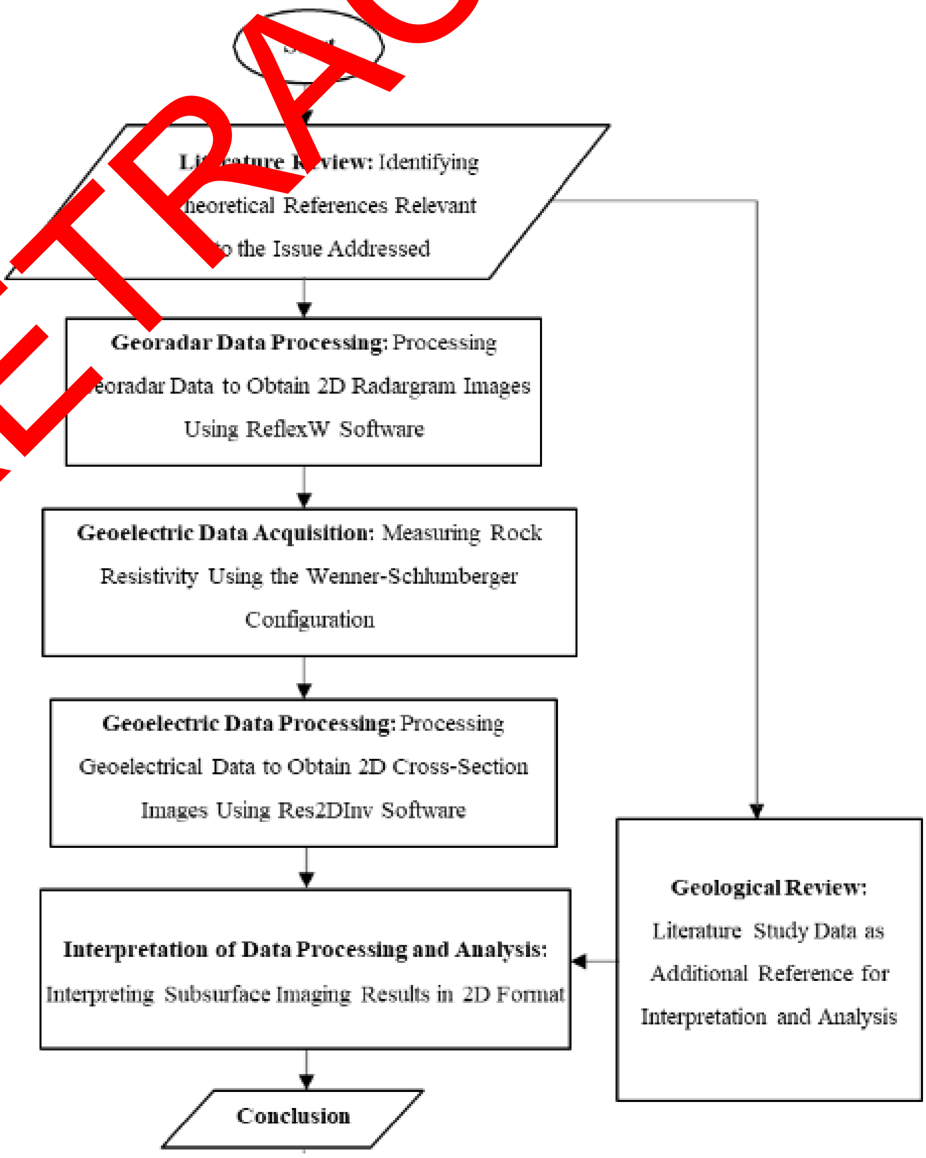

Figure 3. Flow chart of research stages.

2.1 Research Procedures

Geoelectric resistivity data collection in this study used the Wenner-Schlumberger configuration. Measurements were carried out at 4 points with a path length of 34.5 meters for each point with an electrode distance of 1.5 meters. There are only 4 paths taken in this study, namely track

1, track 2, track 3 and track 4. The results of geoelectrical data processing are then used to interpret the results of georadar data processing. The research stages are described in Figure 3.

2.2 Data Processing

2.2.1 Georadar Data Processing

The georadar data processing stage uses ReflexW software to determine the subsurface structure as indicated by differences in layered reflection patterns. The following are the data processing stages depicted in the form of a flow diagram (Figure 4). The advantage of this method is that it can be used to accurately analyze subsurface surface conditions on various types of surface media. This method can be used to analyze the structure of various types of soil such as soil with varying soil density. Apart from that, the georadar method can be used to detect damage to building structures and can be used to detect various minerals or other substances found in the subsurface (Arisona et al., 2023).

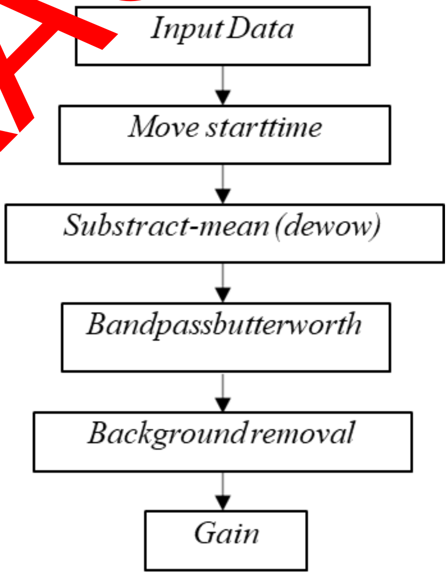

Figure 4. Flow diagram of data processing stages.

2.2.2 Geoelectric Data Processing

From field measurement data, potential difference (ΔV) and electric current (I) values were obtained. Then the apparent resistivity value (ρa) will be calculated using equation (1) (Pratama et al., 2018). Next, an inversion modeling process will be carried out using res2dinv software to obtain the subsurface structure which is indicated by differences in layer resistivity values.

$$\rho_a = n(n+1)\pi a \frac{\Delta V}{I} \quad (1)$$

2.3 Data Interpretation

2.3.1 Georadar Data Interpretation

After carrying out a series of data processing processes with ReflexW software, a radargram image was obtained. To identify subsurface layers based on a radgram, it can be analyzed by looking at certain reflection patterns displayed on the radargram image (Hutasoit & Sumargana, 2023) .

2.3.2 Geoelectric Data Processing

After carrying out a series of data processing processes with res2dinv software, a subsurface cross-section was obtained. Interpretation is carried out by analyzing cross-sections based on resistivity values obtained from data processing results with resistivity values for material types listed in Table 2

(Telford, et al., 1990) and reviewing the geological map of the research area (Figure 5) to determine the types of rocks found in the area. that area. research location.

Table 2 Rock Resistivity Value

No.	Rock Type	Resistivity (Ωm)
1.	Tuff	2×10^3 (*wet*) – 10^5 (*dry*)
2.	Sand	1 – 1000
3.	Sandstone	$1 - 6.4 \times 10^8$
4.	Gravel	100 – 600
5.	Silt	10 – 200
6.	Clay	1 – 100
7.	Pumice	23.9–40 (wet), 204–354 (dry)

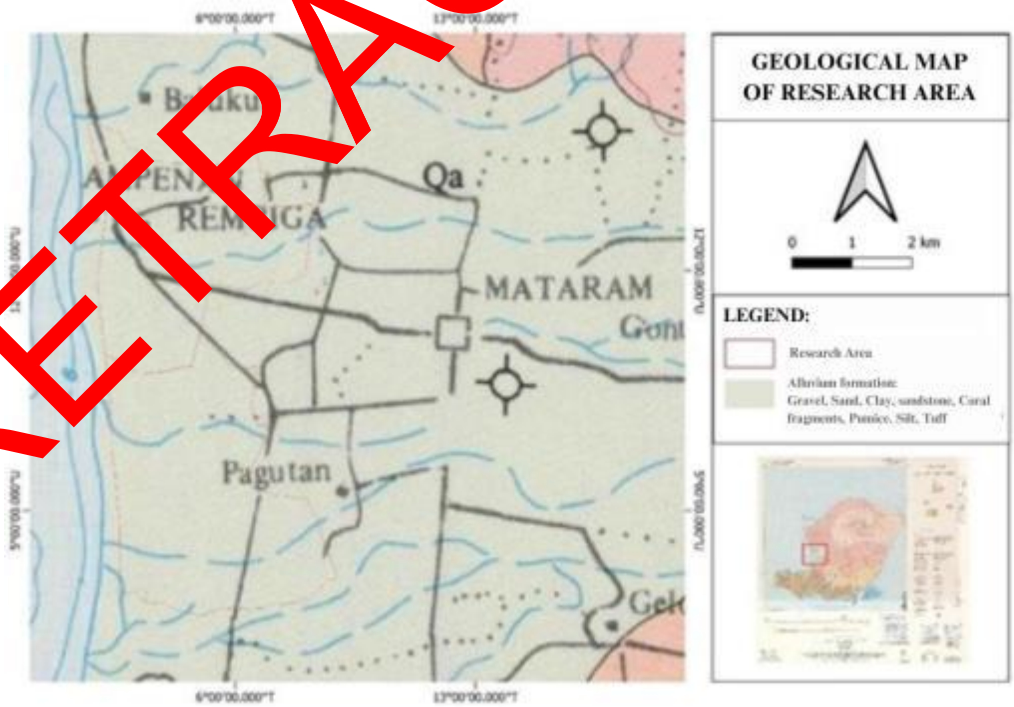

Figure 5. Geological Map of Research Area.

3. RESULTS AND DISCUSSION

This study uses secondary data from georadar and primary data from geoelectric resistivity. Georadar data processing produces radargram images that depict subsurface structures based on changes in reflection signal contrast, while geoelectric resistivity data processing produces 2D cross-sections that show the resistivity distribution below the measurement path. The following are the results of georadar and geoelectric data analysis used to identify the presence of pumice in Ampenan and Sekarbela Districts. There are 4 trajectories in the research location points taken in this study, namely track 1, track 2, track 3, and track 4.

3.1 Track 1

The results of georadar and geoelectric data analysis show the harmony between the radargram image in Figure 6 and the resistivity cross-section in Figure 7. The radargram in series A with a depth of 0 – 9 m which is marked with a purple amplitude shows a wavy reflection pattern, thought to be like a layer of sand. and mud. Furthermore, in series B, a crack zone can be seen at a depth of 9 – 30 m. In the geoelectric cross-section, the layer with a resistivity value of 30.3 – 408 Ωm, marked with light blue to red, is at a depth of 1 – 4.78 m, estimated to consist of a mixture of silt, sand, gravel, clay, and pumice with conditions ranging from wet to dry. This shows that the wavy layer visible on the radargram contains pumice. Based on the results of georadar and geoelectric data analysis, it shows that on Track 1 the pumice stone is at a depth of 1 – 9 meters mixed with silt, sand, and gravel.

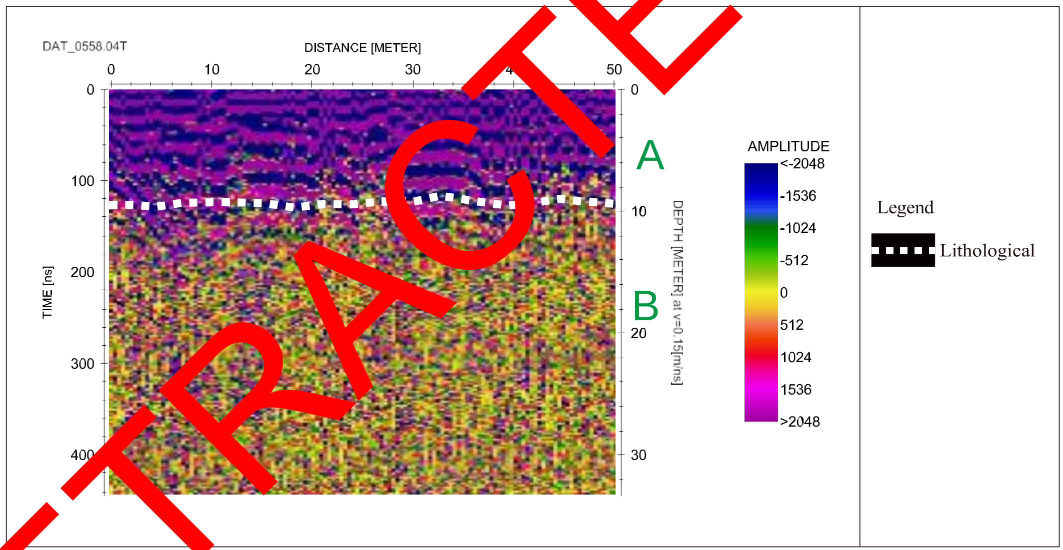

Figure 6. Georadar Data Processing Results on Track 1.

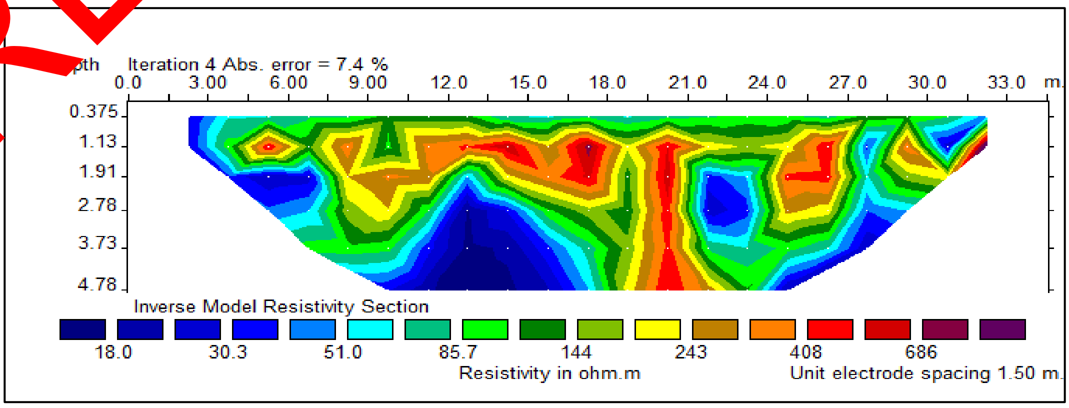

Figure 7. Geoelectric Data Processing Results on Track 1.

3.1 Track 2

The results of georadar and geoelectric data analysis show a harmony between the radargram image in Figure 8 and the resistivity cross section in Figure 9. The radargram in sequence A, with a depth of 0 – 2.3 m, which is marked with a purple amplitude, shows a wavy reflection pattern, estimated as a layer of sand and silt. Furthermore, in sequence B, a crack zone can be seen at a depth of 2.3 – 6.4 m. In the geoelectric cross-section, the layer with a resistivity value of 52.1 – 429 Ωm, marked with dark blue to light green, is at a depth of 1.13 – 4.78 m, estimated to consist of a mixture of silt, sand, gravel, clay and pumice with conditions ranging from wet until dry. This shows that the wavy layer visible on the radargram contains pumice. The layer with a higher resistivity value, namely 866 – 7135 Ωm which is marked with dark green to purple at a depth of 0.375 – 3.73 m, is estimated to be a layer of dry sand and tuff. The presence of crack zones in sequence B, could be related to pressure differences in the soil layers or could also be related to high resistivity variations, indicating the presence of a mixture of dry sand and tuff in the geoelectric section. Based on radargram analysis and geoelectric cross-sections, it can be concluded that on Track 2, pumice is at a depth of 1.13 – 6.4 m, mixed with silt, sand, and tuff.

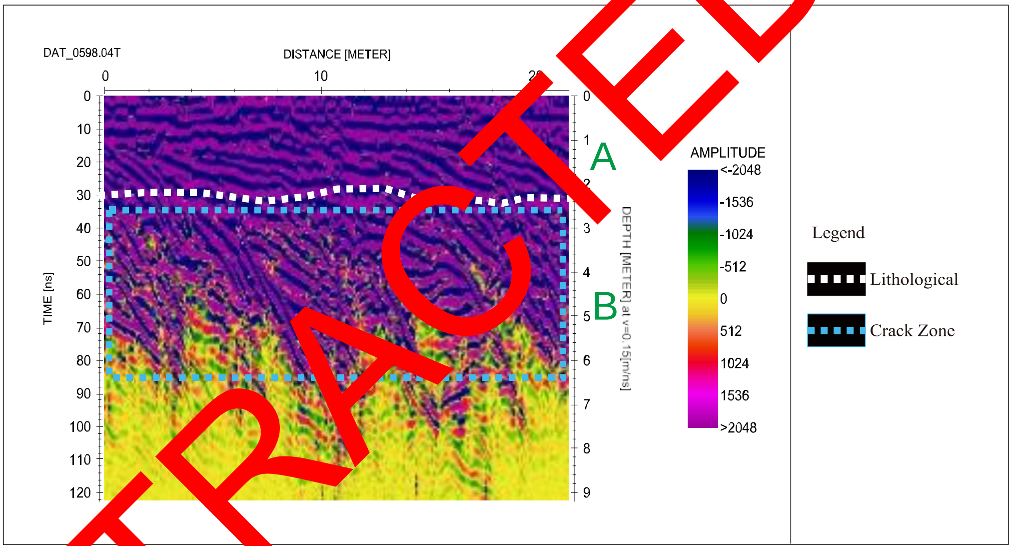

Figure 8. Georadar Data Processing Results on Track 2.

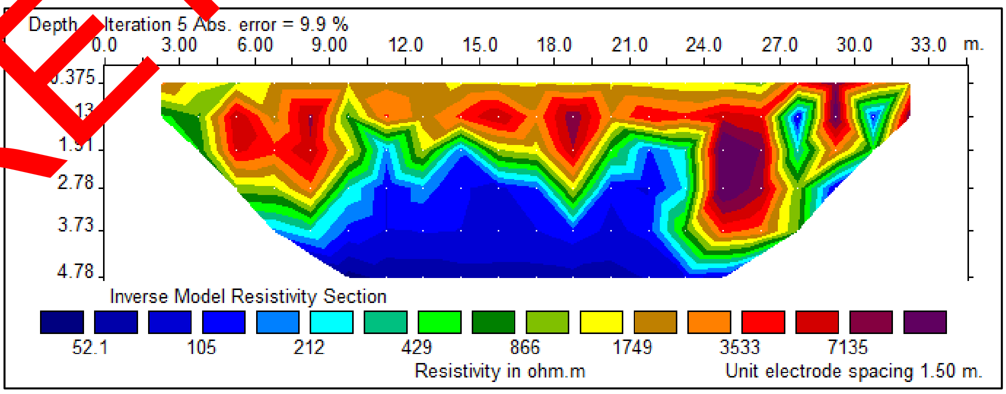

Figure 9. Geoelectric Data Processing Results on Track 2.

3.2 Track 3

The results of georadar and geoelectric data analysis show harmony between the radargram image in Figure 10 and the resistivity cross-section in Figure 11. The radargram in sequence A with a depth of 0 – 1.2 m, which is marked with a purple amplitude, shows a simple layered reflection pattern in a hummocky shape, estimated as a layer of sand and gravel. In the geoelectric cross-section, layers with resistivity values of 45 – 399 Ωm are marked with light blue to red colors at varying depths, ranging from 0.375 – 4.78 m, it is estimated that there is a mixture of sand, gravel, and pumice with wet to dry conditions. This shows that the hummocky layer visible on the radargram contains pumice.

The radargram on sequence B, at a depth of 1.2 – 5.4 m, shows an irregular wave response, the reflection pattern cannot be identified, this could be because the waves have weakened or experienced attenuation due to the conductive layer on sequence B. This finding is in line with the geoelectric cross-section at a distance of 12.5 – 18 m which shows a layer with a low resistivity value of 15.1 – 26.1 Ωm, which is estimated to be sand and clay containing water, marked by a blue layer at a depth of 1.91 – 4.78 m. The influence of water shown on the resistivity distribution in this layer can explain the wave response which has an irregular pattern on the radargram in sequence B.

Radargrams in series C at a depth of 5.4 – 9 m show a chaotic reflection pattern which is thought to be layers of sand and gravel. The existence of chaotic patterns can indicate variations in the composition and structure of subsurface material that are not homogeneous, even though these layers are not directly identified in the geoelectric section. During field data acquisition on Track 3, pumice was found on the surface. This can support the interpretation that the pumice is distributed in shallow layers. The pumice layer which is thought to be in the shallow layer at the measurement location is influenced by human activities, such as excavation and filling of soil.

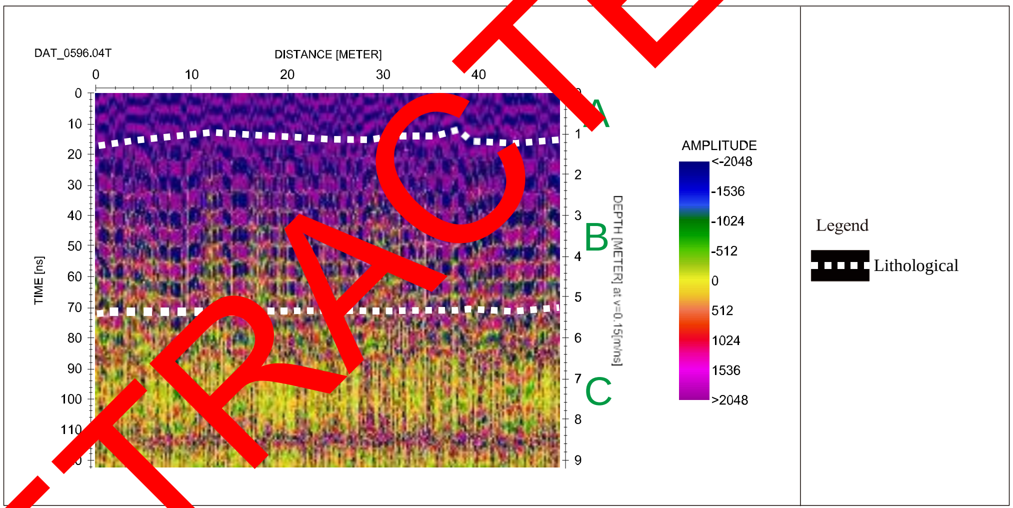

Figure 10. Georadar Data Processing Results on Track 3.

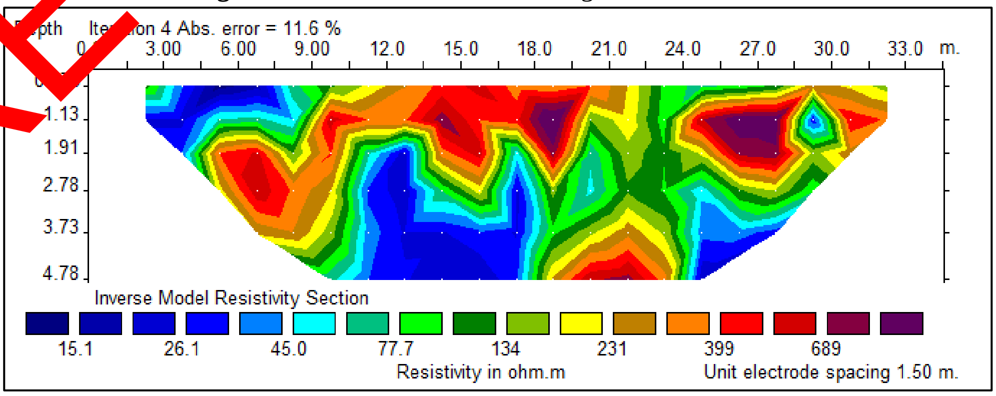

Figure 11. Geoelectric Data Processing Results on Track 3.

3.3 Track 4

The following image is the result of analysis of georadar and geoelectric resistivity data processing on Track 4 located in Pejeruk, Ampenan. The results of georadar and geoelectric data analysis show harmony between the radargram image in Figure 12 and the resistivity cross-section in Figure 13. Radargram in sequence A, with a depth of 0 – 1.89 m, which is marked with a purple amplitude, showing a hummocky reflection pattern, estimated as a layer of gravel and sand. Geoelectric cross sections with resistivity values of 36.4 – 388 Ωm are marked with light blue to orange at varying depths, range 0.375 – 4.78 m, estimated to be a mixture of sand, gravel, pumice, and silt with wet to dry conditions. This shows that the hummocky layer in the radargram contains pumice. This pumice stone was also confirmed by field observations which showed its presence on the surface.

The radargram in sequence B, at a depth of 1.89 – 5 m, shows a combined pattern of parallel and diffraction patterns, whereas the depth increases, the amplitude appears to weaken. Diffraction patterns can be caused by the presence of objects embedded beneath the surface. Meanwhile, the parallel pattern is thought to be layers of wet silt and sand. This is in line with the geoelectric cross-section which shows a low resistivity value, namely 22.7 Ωm, marked in blue at various depths, range 1.13 – 4.78 m, estimated to be a mixture of silt and sand containing water. The influence of water shown on the resistivity distribution in this layer can explain why the radargram in sequence B has a low amplitude as depth increases. Based on radargram analysis and geoelectric cross-sections, it can be concluded that on Track 4, pumice is located at a depth of 0 – 5 m, mixed with silt, sand, and gravel.

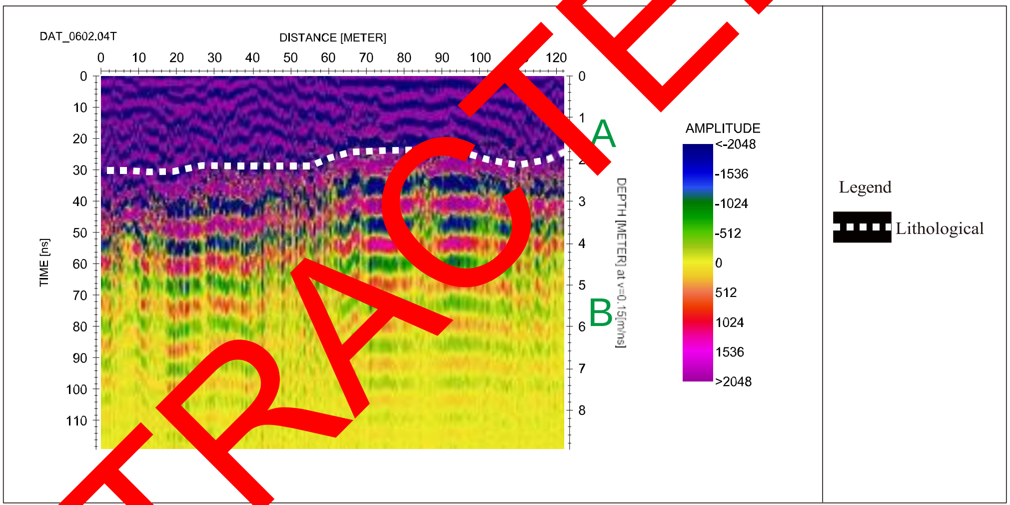

Figure 12. Georadar Data Processing Results on Track 4.

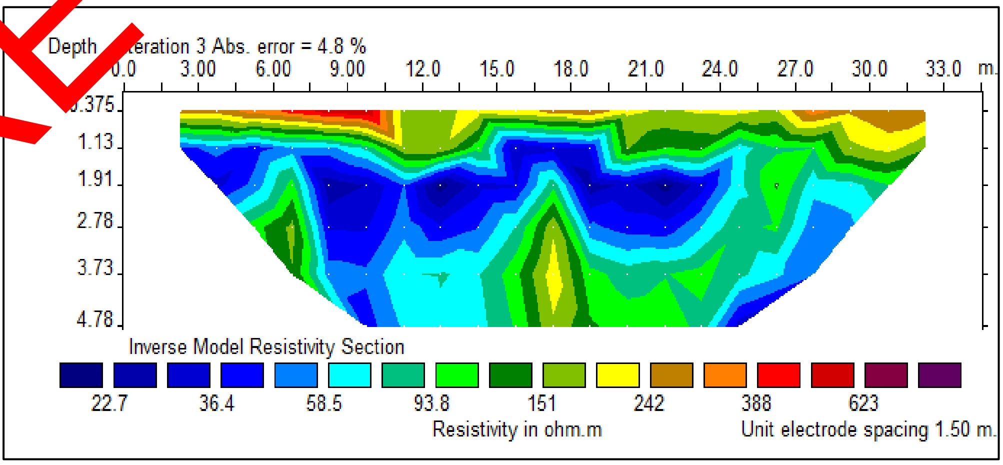

Figure 13. Geoelectric Data Processing Results on Track 4

Radargram images are obtained using the Ground Penetrating Radar (GPR) method, which utilizes electromagnetic waves to reflect differences in conductivity and dielectric properties between subsurface layers. In the radargram, different reflection patterns can be used to identify rock lithology based on changes in physical properties. The physical parameters involved in radargram, and resistivity analysis include the dielectric constant, which measures the material's ability to store electrical energy in an electromagnetic field. Pumice has a low dielectric constant (ε = 2–4) due to its porous structure. Resistivity measures the material's ability to resist the flow of electric current. Dry pumice has high resistivity (≥200 Ωm) due to its non-conductive nature. Overlaying radargrams with geoelectric profiles aims to provide a clearer depiction of lithology by combining information on electromagnetic conductivity and soil resistivity. The first step is data collection, which involves obtaining radargram images from ReflexW software and geoelectric profiles (2D or 3D) from Res2Dinv software. The second step is scaling adjustments, ensuring that the depth scale and radargram track coordinates align with the geoelectric profile. The third step is determining lithological parameters, where radargrams provide reflection patterns that indicate layer boundaries, and resistivity profiles present resistivity values that can be associated with specific rock types. Finally, visual integration is carried out using GIS software to create the overlay, with the radargram imported as the visual base and the resistivity profile layered as a transparent color map. The results of identifying the presence of pumice from the analysis of georadar and geoelectric data on other routes can be seen in Table 3.

Table 3 Results of georadar and geoelectric data analysis

Track	Correlation Results	Depth (m)
1	Silt, sand, gravel, pumice	1 – 9
2	Sand, silt, tuff, pumice	1.13 – 6
3	Sand, gravel, pumice	0 – 4.78
4	Pumice, silt, sand, gravel	0 – 5

Pumice identified in Table 3 refers to fragments distributed within mixed layers as detected by radargram and geoelectric profiles. It may not appear explicitly in the geological map (Figure 5) or as a standalone category in Table 2 due to its secondary distribution.

The results of data analysis in the research area show that the soil layer is dominated by sand, this can be caused by the geographic location of the area which is in a coastal area. On average, pumice is found at a depth of 1 – 6 m, but pumice is also found at a depth of 9 m. The research results obtained from processing georadar and geoelectric data on this measurement line are by with previous research conducted by M[illegible]awani, et al., (2023) and Sudrajat, et al., (2016). The pumice found on the measurement route is not a layer of pure pumice, but only pumice fragments mixed with other materials. This finding is in accordance with research by Ustina, et al., (2020) which states that the thickness of the pumice layer decreases exponentially as the distance from the eruption source increases. The results of data analysis also show that the research area has a shallow groundwater level, where the rock layer above the groundwater level consists of gravel, sand, pumice, and tuff. This is also in accordance with the results of the reconstruction of drill log data from Musa, et al., (2019) which shows that the type of lithology above the aquifer that makes up Mataram City consists of alluvial deposits, sand, pyroclastic and volcanic rock.

As a light volcanic material, pumice often accumulates on the surface of the ground or in shallow layers after being carried by wind and water after volcanic eruptions. This accumulation contributes to the characteristic soil composition of coastal areas, where sand and pumice are often found together. Pumice stone is not a conductive material, so it has a high resistivity value. The porous structure of pumice makes it less efficient at conducting electricity. This research strengthens understanding of the distribution and composition of volcanic material in the study area, as well as providing a more detailed picture of the local geological characteristics.

4. CONCLUSION

Based on the results of georadar and geoelectric data analysis, it shows that the pumice stone resulting from the eruption of Mount Samalas is spread throughout the measurement route with a depth of 0 – 9 m. Data shows that pumice is distributed in the form of fragments mixed with other materials such as gravel, silt, tuff, clay, and fine to coarse sand. Research results also show that volcanic materials such as pumice often accumulate on the surface or in shallow layers. The results of data analysis in the research area show that the soil layer is dominated by sand, this can be caused by the geographic location of the area which is in a coastal area. On average, pumice is found at a depth of 1 – 6 m, but pumice is also at a depth of 9 m.

ACKNOWLEDGEMENT

I would like to thank the Physics Study Program at FMIPA, Mataram University, and the Physics Study Program at FMIPA, Bengkulu University, for their invaluable assistance in completing this study.

REFERENCE

Amin, M., Tambun, B., & Halawa, A. (2023). Identifikasi lapisan aquifer berdasarkan metoda geolistrik konfigurasi Wenner Schlumberger di Desa Petuaran Hilir Kecamatan Pegajahan Kabupaten Serdang Bedagai. *Jurnal Teknologi Informasi Dan Industri*, *3*(2), 1[illegible]7–177.

Arisona, Fiqriawan, M. R., & Safiuddin, L. O. (2023). Pemanfaatan Metode Georadar dalam Menganalisis Lapisan Tanah di Indonesia. *Einstein's: Research Journal of Applied Physics*, *1*(2), 38–41. https://doi.org/10.33772/einsteins.v1i2.154

Hutasoit, B. S. R., & Sumargana, L. (2023). Identifikasi Ketebalan Gambut Berdasarkan Parameter Kecepatan dan Amplitudo Gelombang Menggunakan Metode Refilling GPR. *Prisma Fisika*, *10*(3), 222. https://doi.org/10.26418/pf.v10i3.57790

Ibrahim, E., Imam, S., & Bhinneka. (201[illegible]). Identifikasi Arah Aliran Bawah Permukaan Dengan Metode GPR(Ground Penetrating Radar). *Seminar Nasional Hari Air Sedunia*, 2(1), 123–132.

Lavigne, F., Degeai, J. P., Komorowski, J. C., Guillet, S., Robert, V., Lahitte, P., Oppenheimer, C., Stoffel, M., Vidal, C. M., Suronoh, Pratomo, I., Wassmer, P., Hajdas, I., Hadmoko, D. S., & De Belizal, E. (2013). Source of the great A.D. 1257 mystery eruption unveiled, Samalas volcano, Rinjani Volcanic Complex, Indonesia. *Proceedings of the National Academy of Sciences of the United States of America*, *110*(42), 16742-16747. https://doi.org/10.1073/pnas.1307520110

Malawani, M. N., Lavigne, F., Hadmoko, D. S., Syamsuddin, S., Handayani, L., Sudrajat, Y., Virmoux, C., Saulnier Copard, S., & Kusnadi, K. (2023). Coastal sedimentation and topographic changes in the Mataram Plain, Lombok (Indonesia) following the 1257 CE eruption of Samalas volcano. *Earth Surface Processes and Landforms*, *48*(10), 2100-2116. https://doi.org/10.1002/esp.5592

Narotama, [illegible]arjan, A. F., & Muchtaranda, I. H. (2023). Kajian Geoteknik Bawah Permukaan Dengan Menggunakan Pendekatan Metode Geofisika. *Jurnal Pendidikan, Sains, Geologi, Dan Geofisika (GeoScienceEd Journal)*, 4([illegible]), 1[illegible]. https://doi.org/10.29303/goescienceedu.v4i1.217

P[illegible]bonan, A. ya[illegible], Nugraha, P., Santoso, N. A., Firdaus, R., Ekawati, G. M., Rahmanda, V., & Amijaya, F. D. [illegible]. (202[illegible]). Investigasi Air Tanah Berdasarkan Nilai Lampung Selatan Groundwater Investigation Based on the Resistivity Value in Jatisari Village , South. *Jurnal Geofisika Eksplorasi*, *07*(02), 100–110. https://doi.org/https://doi.org/10.23960/jge.v7i2.117

Pr[illegible]ma, R. K., Akmam, & Mahrizal. (2018). Identifikasi Prekursor Tanah Longsor Berdasarkan Perubahan Nilai Tahanan Jenis Batuan Menggunakan Metode Geolistrik Time-Lapse Konfigurasi Dipole-Dipole Di Bukik Lantiak Kecamatan Padang Selatan. *Pillar of Physics*, *11*(1), 41–48.

Ronodirdjo, M. Z., Syamsuddin, S., Sukrisna, B., Ayub, S., & Taufik, M. (2020). Studi Sejarah Letusan Samalas Berdasarkan Stratigrafi Endapan Vulkanik di Daerah Gangga, Lombok Utara. *Jurnal Pendidikan, Sains, Geologi, Dan Geofisika (GeoScienceEd Journal)*, *1*(1). https://doi.org/10.29303/goescienceedu.v1i1.30

Sudrajat, Y., Handayani, L., Hananto, N. D., Mutaqin, B. W., Lavigne, F., Nyanjang, N., & Sutarman, S. (2017). Pengukuran Geolistrik Untuk Memetakan Cekungan Airtanah Di Kota Mataram. *Prosiding Geoteknologi LIPI*, 1–14.

Tranggono, A., Salim, A., Leda, J., & Rauf, I. (2024). Korelasi Kadar Air Tanah dan Nilai Geo- Resistivitas Metode Geolistrik. *Journal of Science and Engineering*, *7*(1), 12-18.

Ustina, Y., Sukrisna, B., & Hiden, H. (2020). Analisis Ketebalan Lapisan Batu Apung Fungsi Jarak Dari Sumber Menggunakan Metode Geolistrik Resistivitas di Kecamatan Lingsar, Lombok Barat. *Indonesian Physical Review*, *3*(2), 53-63. https://doi.org/10.29303/ipr.v3i2.41

Vinod, C. T. (2014). Geotechnical Applications of Ground Penetrating Radar (GPR). *Jour. Ind. Geol. Cong.*, *6(1)*, 35-46.

Wahidah, A. N., Rachmat, H., Rosana, M. F., Rinjani, G., Aikmel, K., & Lombok, K. (2016). Petrogenesis Batuan Piroklastik Gunung Rinjani. *Proceeding, Seminar Nasional Kebumian Ke-9 Peran Penelitian Ilmu Kebumian Dalam Pemberdayaan Masyarakat, Grha Sabha Pramana*, 433–444.